Climate Change and Invasion Expansion Jointly Reshape Geographic Ranges of Invasive Tephritid Fruit Flies

Zihua Zhao (zhzhao@cau.edu.cn)
China Agricultural University https://orcid.org/0000-0003-2353-2862

Yu Zhang
China Agricultural University

Gonzalo A Avila
New Zealand Institute for Plant and Food Research Mount Albert Campus: New Zealand Institute for Plant and Food Research Ltd

Peng Han
Sichuan University - Wangjiang Campus: Sichuan University

Xubin Pan
Chinese Academy of Inspection and Quarantine

Yujia Qin
China Agricultural University

Zhihong Li
China Agricultural University

Gadi V.P. Reddy
USDA-ARS-SRRC: USDA-ARS Southern Regional Research Center

Mark van Kleunen
Universität Konstanz: Universitat Konstanz

Cang Hui
Stellenbosch University

Research Article

Keywords: Biological invasions, invasion dynamics, non-native species, Oriental fruit fly, occurrence probabilities, global warming

Posted Date: July 29th, 2021

DOI: https://doi.org/10.21203/rs.3.rs-733983/v1

Climate change and invasion expansion jointly reshape geographic ranges of invasive tephritid fruit flies

Zihua Zhao[1,*], Yu Zhang[1], Gonzalo A Avila[2], Peng Han[3], Xubin Pan[1], Yujia Qin[1], Zhihong Li[1], Gadi V.P. Reddy[4], Mark van Kleunen[5], Cang Hui[6,7]

[1] Department of Plant Biosecurity, College of Plant Protection, China Agricultural University, Beijing 100193, China;

[2] The New Zealand Institute for Plant & Food Research Limited, Private Bag 92169, Auckland 1142, New Zealand;

[3] Laboratory of Ecology and Evolutionary Biology, Yunnan University, Kunming 650504, Yunnan, China;

[4] USDA-ARS-Southern Insect Management Research Unit, 141 Experiment Station Road, PO Box 346, Stoneville, MS 38776, USA;

[5] Department of Biology, University of Konstanz, Konstanz 78464, Germany;

[6] Department of Mathematical Sciences, Centre for Invasion Biology, Stellenbosch University, Matieland 7602, South Africa;

[7] Mathematical and Physical Biosciences, African Institute for Mathematical Sciences, Muizenberg 7945, South Africa.

Corresponding author: zhzhao@cau.edu.cn (ZZ), +86-0162732068 (TEL)
Other email: zhangyu@alu.cau.edu.cn; gonzalo.avila@plantandfood.co.nz; penghan1394@163.com; xubin.hu.pan@gmail.com; qinyujia@cau.edu.cn; lizh@cau.edu.cn; gadi.reddy@usda.gov; mark.vankleunen@uni-konstanz.de; chui@sun.ac.za

Abstract: Human-mediated species introductions have greatly contributed significantly to the current global alteration of the biosphere, with many invasive species rapidly expanding their geographic ranges, leading to changes in biodiversity and disruptions of ecosystem functioning. With a modified SDM that considers both extensive data coverage and the distance to previously already occupied areas, we show continued shifts and expansions of geographic ranges of two globally invasive tephritid pest species *Bactrocera dorsalis* and *Ceratitis capitata*). Both tephritid pests are still expanding globally, with their geographic ranges estimated to have expanded by 65% and 22% in the past three decades. The potential future geographic distributions of *B. dorsalis* and *C. capitata* under four scenarios of Representative Concentration Pathways (RCPs) for 2050 highlighted some key changes when compared to their current occurrences. Under all four RCPs by 2050, the potential geographic distribution of *C. capitata* was predicted to shrink by 5-14%, while the distribution of *B. dorsalis* was predicted to increase by 12-15%. Under different climate scenarios for 2050, *B. dorsalis* could experience a notable poleward expansion with increasing connectivity in its future geographic distribution. The two tephritids will continue to co-occur in Africa, with *B. dorsalis* experiencing higher suitability in most regions where they overlap. Climate changes were estimated to contribute more, than non-equilibrial invasion expansion, to changes in the geographic ranges of the two tephritid pests. The forecasted potential geographic distributions could enhance regional biosecurity preparedness in future climates and mitigate proactively the economic loss from these fruit fly pests.

Key words: Biological invasions, invasion dynamics, non-native species, Oriental fruit fly, occurrence probabilities, global warming.

Introduction

The spread of non-native organisms has been drastically on the rise over the last century, arguably accelerated by ongoing global climate change. Indeed, climate change has altered global gradients in environmental factors such as temperature and precipitation, and increased the frequency of extreme events (Urvois et al. 2021; Simberloff et al. 2013). These alterations of environmental gradients often drive range shifts in both native and non-native species, reducing ecosystem resistance and resilience to further invasions (Hulme 2006).

Invasive pest species have been increasing at an unprecedented rate in agricultural ecosystems worldwide in recent decades (Seebens et al. 2019). Although many insect species are not considered as pests in their native habitats, some can cause serious ecological and economic impacts once established in other regions (Diagne et al. 2021). For example, most tephritid fruit flies are part of the non-pest components of native biota (Aluja and Mangan 2008), but some have become important global invasive pests that feed on a wide range of fruits and vegetables. These pests include the Oriental fruit fly (Orifly), *Bactrocera dorsalis* (Hendel) and the Mediterranean fruit fly (Medfly), *Ceratitis capitata* (Wideemann) (both species belongs to Diptera: Tephritidae), which both can be easily transported as larvae or pupae in infested fruits. Orifly originated in the tropical area of Asia and to date has invaded many parts of Africa, Oceania, Europe, North America, and West Australia (Zeng et al. 2019). Medfly originated in Africa and has spread to South America, North America, and Europe (Vera et al. 2002). Before 2020, Medfly and Orifly had already been transported to more than 70 and 100 countries, respectively, and both species are listed as important quarantine insect pests by the USA, Australia and China (De Meyer et al. 2008; Zeng et al. 2019). Countries with invasive tephritid pests have suffered export restrictions on their fruit products, requiring costly quarantine

treatments before export (Follett and Hennessey, 2007; Holmes et al. 2010; Beaury et al. 2020). Furthermore, the co-invasion by Orifly and Medfly has caused infestations of multiple fruits and agricultural products especially in Africa. Intriguingly, the Orifly and Medfly, which share the same hosts, have co-invaded some areas (e.g., Kenya and parts of Africa), resulting in severe economic loss due to mixed infestation (Hussain et al. 2015).

Invasive species typically have not fully explored their niche opportunities in the invaded range and are thus experiencing non-equilibrial invasion dynamics (Hui and Richardson 2017). Consequently, for risk assessment and management planning, it is essential to consider the role of invasive spread (Low et al. 2021) when forecasting the potential geographical distribution (PGD) of non-native organisms. That is, invasion risk is a composite result of both habitat suitability and the likelihood that it will arrive from already occupied areas (Bertelsmeiera et al. 2018; Williams et al. 2021).

The acceleration of global warming will likely further shift or even expand the PGDs of non-native species (Cornelissen et al. 2019; Thomas 2010). Climate change, especially global warming, may make these remaining areas also suitable for these two invasive fruit flies, exacerbating their global progression into currently uninvaded areas (Zhao et al. 2020). Species distribution models (SDMs), also called ecological niche models, are classic techniques for estimating habitat suitability and the PGD of non-native species (Elith et al. 2011). It is an effective method to identify suitable but unoccupied areas that could also emerge in future climates and thus face potential invasion risks of non-native species (Godefroid et al. 2020; Pouteau et al. 2021). A key challenge to this method is model transferability when predicting species distributions in novel environments (Peterson et al. 2007). Such models normally rely on realized niches (species-environment relationships), together with occurrence records and environmental data, and can project the joint effects of dispersal, biotic

interactions, and environmental filtering (Peterson et al. 2011; Puchałka et al. 2021).

By assessing the likely changes in the PGDs of Orifly and Medfly, we can examine the relative sensitivity of predicted invasion risks of these non-native species under different climate change scenarios (Kriticos et al. 2017). Here, we use a modified procedure of SDMs that considers both factors of climate change and arrival probability and assess the current and future PGDs of Orifly and Medfly under different climate conditions. We explore the potential invasion risks and processes of these species in both co-occurring and separately occurring areas. This study provides an early warning signal for collective management by identifying future susceptible regions to the invasions of these two globally invasive fruit fly pests (Maino et al. 2016).

Methods

Occurrence and bioclimatic data

Current geographical distribution data for both Orifly and Medfly were compiled from existing databases, including the CABI Invasive Species Compendium (www.cabi.org/isc; retrieved on Febrary-17-2020), the Global Biodiversity Information Facility (www.gbif.org; retrieved on January-15-2020) and the literature (De Meyer et al. 2008; De Villiers et al. 2016; Stephens et al. 2007; see Table S1). We classified all occurrence records into three categories: presence, absence or eradicated in a particular year. A ‘presence’ record represents a confirmed detection or a positive finding after an eradication program. An ‘eradicated’ record represents a negative finding from surveillance after an eradication program. An ‘absence’ record represents no further detections after continuous surveillance after having been reported of a temporary presence but without any specific eradication

programs. For the species distribution modelling (see below), we only used data of 'presence' records. In particular, for each tephritid species, we created a binary raster map of infestation, in which each infested grid cell (approximates 50 by 50 km in size (0.5° by 0.5°)) could have more than one presence record. Globally, we have 838 and 622 infested cells for Orifly and Medfly, respectively, covering a period from 1900 to 2020 (Figure 1, S1 and S2).

Past and future bioclimatic data were extracted from the WorldClim database (version 2.1; www.worldclim.org) at a resolution of 50 by 50 km under the Behrmann Equal Area Cylindrical projection. We used the future climate data for 2050 that includes the average of 2041 to 2060 predictions of the earth system model MIROC-ESM-CHEM (MI) under four representative concentration pathways (RCP2.6, RCP4.5, RCP6.0 and RCP8.5), representing future scenarios of low to high greenhouse gas emissions (Meinshausen et al. 2011). To identify bioclimatic variables that are strongly collinear, we did principal component analyses and pairwise correlation analyses in SPSS 20 (Table S2).

To optimize the environmental variables, a back and forth, stepwise method was used to screen the bioclimatic variables. The variables with a high contribution rate (>0.8) were selected to conduct further model analyses. Specifically, we selected temperature (temperature seasonality, mean temperature of warmest quarter, and mean temperature of the coldest quarter) and precipitation (precipitation of the wettest quarter and precipitation of the driest quarter) for the subsequent species distribution modelling. These selected environmental variables have been widely used as important drivers of the physiological performance and thus population dynamics for insects (Puchałka et al. 2021).

Dynamic species distribution modelling

We used the well-developed species distribution model (SDM) Maxent but followed a novel procedure to explore the range dynamics. Maxent is a machine learning algorithm for predicting the PDGs with presence-only records. A large number of publications have been dedicated to explain, test and improve Maxent in species distribution modelling (e.g., Pearson et al. 2007; Phillips and Dudik 2008; Elith et al. 2011; Warren and Seifert 2011; Merow et al. 2013; Muscarella et al. 2014). Specifically, we used Maxent v3.3.3k (www.ipp.mpg.de/maxent2019) for predicting the PGDs of Orifly and Medfly.

We first prepared the Orifly data based on accumulated 'presence' records for three periods: 1900-1960, 1960-1990, 1990-2020, denoted as $y_{1960}^{i,o}$, $y_{1990}^{i,o}$ and $y_{2020}^{i,o}$, respectively, for grid cell i. We then created a spatial layer using the Spatial Analyst function of ArcGIS10.2, representing the distance between grid cell i to the nearest presence records (distance to infested area) in the three presence layers, denoted as $d_{1960}^{i,o}$, $d_{1990}^{i,o}$ and $d_{2020}^{i,o}$. Similarly, we define the variables of the Medfly (e.g. $y_{1990}^{i,m}$ and $d_{2020}^{i,m}$). We also prepared the layers of each bioclimatic variable (See Table S1) for each of the three periods ($x_{j,1960}^{i}$, $x_{j,1990}^{i}$, $x_{j,2020}^{i}$).

In a typical Maxent analysis, the model explains the presence records (y^i) by a set of explanatory variables (x_1^i, x_2^i, …) and predicts the occurrence probability (e.g. $p_{1990}^{i,o}$) as the model output:

$$p_{1990}^{i,o} = \mathrm{Maxent}(y_{1990}^{i,o} | x_{1,1990}^{i}, x_{2,1990}^{i}, \dots). \quad (1)$$

Effectively, this is an estimate of habitat suitability, whereas the occurrence probability at a location might additionally depend on how likely it is that the species will arrive there. The latter is likely to depend on how distant the location is to currently occupied locations. Moreover, the occurrence

probability of a species could depend on the distribution of other species that may interfere with it. Therefore, we added to two distance predictors to the Maxent model.

That is, we followed an alternative procedure to predict the occurrence probability of Orifly for two periods:

$$p_{1990}^{i,o} = \text{Maxent}(y_{1990}^{i,o} | d_{1960}^{i,o}, d_{1960}^{i,m}, x_{1,1990}^{i}, x_{2,1990}^{i}, \dots), \quad (2)$$

$$p_{2020}^{i,o} = \text{Maxent}(y_{2020}^{i,o} | d_{1990}^{i,o}, d_{1990}^{i,m}, x_{1,2020}^{i}, x_{2,2020}^{i}, \dots). \quad (3)$$

The contribution of $d_{1960}^{i,o}$ in Maxent model (2) represents the contribution of distance to infested area (invasion expansion) from 1960 to 1990 in the geographic range of Orifly; $d_{1960}^{i,m}$ the interference from Medfly, if any, to the range changes in Orifly (Medfly and Orifly share the same niche of host ranges); $x_{j,1990}^{i}$ the contribution of climate characteristics in variable j to the geographical distribution of Orifly. The fitted model (3) was then used to predict the occurrence probability in 2050:

$$p_{2050}^{i,o} = \text{Maxent}(\_ | d_{2020}^{i,o}, d_{2020}^{i,m}, x_{1,2050}^{i}, x_{2,2050}^{i}, \dots). \quad (4)$$

Similarly, we also modelled the occurrence probability of Medfly ($p_{1990}^{i,m}$, $p_{2020}^{i,m}$ and $p_{2050}^{i,m}$). The Jackknife method was selected for measuring the contribution of different predictors in the model to occurrence probability; a receiver operating characteristic (ROC) curve, averaged over multiple runs, was calculated, and the area under the ROC curve (AUC) was used for model performance evaluation (Radosavljevic and Anderson 2014).

Post-SDM analyses

Occurrence probabilities predicted from the Maxent model were converted into raster files using ArcGIS10.2. For better discussion and visualization, we divided the model predictions of occurrence probability ($p^{i,o}$ and $p^{i,m}$) into four levels: negligible (0.00-0.10), low (0.10-0.25), medium (0.25-0.50) and high (0.50-1.00). The area and perimeter of the PGDs in each continent (defined for occurrence probability ≥ 0.1) were calculated using Spatial Analyst in ArcGIS10.2 under the Behrmann Equal Area Cylindrical projection. For each continent, we calculated the relative change in the area and connectivity of PGDs from 2020 to 2050. In particular, we calculated the relative change in the area with occurrence probability ≥ 0.1 (e.g. for Orifly):

$$\Delta P^{o}_{2050} = (P^{o}_{2050} - P^{o}_{2020})/P^{o}_{2020} \quad (5)$$

Connectivity depicts the functional relationship among habitat patches of PGDs and was calculated as the perimeter divided by the area, $C^{sp}_{year} = \text{Perimeter}(p^{sp}_{year} \geq 0.10)/\text{Area}(p^{sp}_{year} \geq 0.10)$. Thus, the relative change in PGD connectivity can be calculated as:

$$\Delta C^{o}_{2050} = (C^{o}_{2050} - C^{o}_{2020})/C^{o}_{2020} \quad (6)$$

The co-occurring PGDs of Orifly and Medfly were estimated using the Intersect and Symmetrical Difference tool in ArcGIS10.2. The occurrence probabilities of Orifly and Medfly in the co-occurring areas were compared to indicate potential local dominance by one tephritid species. The species with the highest occurrence probability is assumed to be dominant in our analysis. In addition, we tested the fixed effect of different RCPs on predicted occurrence probability ($p^{i,}_{2050}$) with a generalized linear mixed model (GLMM) with continents as the random effect, using the function *glmer* from the package 'lme4' (Bates et al. 2015) in R 4.0.3 (R Core Team 2016).

Results

Distribution records

As of 2020, Orifly has currently infested 72 countries in South Asia and Africa. It is still largely absent from South America (Fig. 1a, Table S1) but it has been repeatedly detected in Chile since 2014. It was already widely distributed in Southeast and South Asia before 2000. Orifly invaded Africa in 2006 and has since been rapidly expanding across the continent (Fig. 1b, Fig. S1a-f). Most of the 12 newly invaded countries in the past decade (2010-2020) are African nations. However, invasive Orifly populations have been effectively eradicated in the USA, Australia and Japan (Fig. 1a). The native range of Medfly is West Africa. It invaded Spain in 1842 and subsequently spread to South America in 1930 (Fig. S2a-f). At present, it is mainly distributed in Europe, Africa, as well as Central and South America, with 101 countries having confirmed cases (Fig 1c). Although Medfly is largely absent in Asia, it has expanded rapidly in Africa, Europe and South America during the past several decades (Fig 1d, Table S1). The two species currently co-occur in Africa and Hawaii. Until 2020, both tephritid species were still expanding globally, with Orifly still at a high rate, while Medfly close to saturation (Figure 1b and d).

Model performance

All five selected bioclimatic variables and distance to the most adjacent conspecific record (representing invasive spread) were chosen for the Maxent modelling of Orifly (Fig. 2a-f). For Medfly, mean temperature of the coldest quarter was dropped from the models due to trivial contribution (Fig. 2). Similarly, interspecific interference (i.e. distance to the most adjacent record of

the other species) was also dropped. The Maxent models for both tephritid pests performed well (AUC > 0.9; Fig. S3a-d). Among the bioclimatic variables, precipitation of the wettest quarter was found to contribute the most to explain the occurrence probability of Orifly (Fig. S3a-b), while temperature seasonality was the most important predictor of Medfly occurrence probability (Fig. S3c-d). For both 2020 and 2050, according to regularized training gain, temperature seasonality, mean temperature of warmest quarter, precipitation of the wettest quarter, and distance to infested area contributed most to predicting occurrence probabilities of Orifly (Table S3). The same variables, with the exception of precipitation of the wettest quarter, also contributed most to occurrence probabilities of Medfly (Table 1). The predicted occurrence probabilities of Orifly were overall greater than those of Medfly under high temperatures (Figure 2b). The PGDs for both Orifly and Medfly were greatly mediated by invasion expansion (i.e. distance to the most adjacent conspecific record in the past three decades) (Table S3 and Figure 2).

Current and future distributions

Range shifts of PGDs in Orifly during 1990-2020 were well explained by invasion expansion from distance to the areas that were already infected in 1960-1990 (Fig. 3a, b; Table S3). Orifly has the largest PGD (1,486 million ha) in South America under the current climatic conditions, with 15.3% of the predicted PGD (for $p_{2020}^{i,} > 0.1$) in this continent highly suitable ($p_{2020}^{i,} > 0.5$; Table S4). There are also large PGDs for Orifly in North America (286 million ha), particularly in Mexico, California and Florida (Fig. 3b). Under RCP 8.5 (a scenario of high greenhouse-gas emissions), the PGD of Orifly would increase by 3% by 2050 in all continents (excluding Antarctica). Importantly,

the percentage of highly suitable area would increase by up to 50% in Asia, Africa and South America (Fig. 3c). The predicted PGDs of Orifly in 2050 are visually similar to each other under the four RCP scenarios (Figs. 3a-c, Fig. S4). Moreover, under climate scenario RCP 8.5, Orifly could experience a notable poleward expansion (Fig. 4a), although its distribution in the Middle East was predicted to shrink slightly; similar poleward expansions were also predicted under other milder climate change scenarios (RCP 2.6, 4.5, and 6.0; Fig. S5). Overall, the worldwide PGD of Orifly was predicted to have increased by 12-15% in 2050 (Table S6, Fig. S6a).

The PGDs of Medfly in 1990 was also a good predictor of its distribution during 1990 to 2020 (Table 1, Fig. 3d, e). Under the current climatic condition, 42.1% of the predicted PGD in Asia is of medium or high suitability ($p_{2020}^{i,} > 0.25$; Table S5). In the southern USA and Mexico, Medfly was estimated to have an extensive suitable range (556 million ha, $p_{2020}^{i,} > 0.1$; Fig. 3e). The PGDs of Medfly in South America, Africa and Oceania were predicted to shrink and become more fragmented (Fig. 4b; connectivity to decline 85% by 2050). For instance, under RCP 8.5, the highly suitable areas for Medfly were predicted to shrink by 2% in Africa and 3% in South America by 2050 (Fig. 3f). The worldwide PGD of Medfly was predicted to decrease by 5-14% in 2050, expanding only in North America and Europe (Fig. 5, Fig. S6a and b, Table S6 and S7).

Co-occurrence

Under various climate change scenarios, Orifly and Medfly were predicted to jointly occur in many areas of their current and future PGDs than they currently do (Figs. 6a-b). In these areas of potential co-occurrence, Orifly dominance (higher occurrence probability) was 16% larger than Medfly

dominance. Under RCP 8.5 in 2050, Orifly dominance regions were predicted to increase by 29% in Africa and 39% in South America due to greater occurrence probabilities in higher temperature regions than Medfly (Fig. 2b). In Europe, Medfly was predicted to be dominant over Orifly in 58% of the areas of predicted co-occurrence under future climate change scenarios. In contrast, Orifly could be dominant in 71% of the potential co-occurrence areas in Asia, while Medfly only in 7% under RCP 8.5 in 2050. Under other milder climate-change scenarios (RCP 2.6, 4.5, 6.0), Orifly was predicted to be still dominant in more areas of potential co-occurrence than Medfly in South America, Africa, and Asia (Table S8).

Discussion

Both tephritid pests have globally expanded their geographic ranges in the past several decades. We here showed that with further climate changes and invasion expansion, the PGDs of Medfly are predicted to expand in Europe and North America and to shrink in other continents. Furthermore, both species are still expanding their potential areas of high occurrence probability (habitat suitability), fuelling ongoing invasions and recurrences. Under future climate, South America and Asia would be highly vulnerable to invasions by Orifly and Medfly, respectively.

Global warming, coupled with spread from the nearby already infected areas, will significantly enhance the ability these tephritid pests to expand their geographic distribution. The risks and impacts of these tephritid pests are also likely to increase due to climate change (Vera et al. 2002; Szyniszewsha and Tatem 2014). Orifly will benefit more than Medfly from global warming, because Orifly has a higher optimal performance temperature: the occurrence probability of Medfly peaked at

31°C in the warmest quarter, in contrast to 34°C for the occurrence probability of Orifly. This explains why Orifly is expected to undergo large geographic expansion in a warming world (Hill et al. 2016), and especially so in tropical regions (Armstrong et al. 2009).

Co-invasions of fruit flies have occurred in Africa and America, and could be a common phenomenon for tephritid invasions as several individuals of multiple tephritid species often infest the same orchards (Rodriguez-Rodriguez et al. 2018) and even fruits (Pieterse et al. 2020; Ganie et al. 2013). Indeed, the co-habitation of Orifly and Medfly in a single fruit has been reported in cases from Hawaii and Africa (Haramoto and Bess 1970; Hussain et al. 2016).

When estimating the PGD of an invasive species, it is essential to consider diverse predictors that can affect the target species' recruitment and dispersal (Taylor and Kumar 2012). The previous research also revealed that the PGDs of tephritid pest would be a critical indicator of invasion expansion (Szyniszewska and Tatem 2014; De Villiers et al. 2016). Our prediction considered both bioclimatic conditions, invasion expansion from adjacent occupied areas, and interferences from other species by using the extensive data coverage and the distance to previously already occupied areas. An immediate improvement of our model is to include host distributions and fruit trade networks as covariates, which could change the roles of bioclimatic conditions and invasion expansion, as well as predicted PGDs of these tephritid species (Zhao et al. 2019).

Conclusion

Both Orifly and Medfly have expanded their geographic ranges substantially in the past century through successful invasions of new regions, despite quarantines, eradication programs, and

suppressive management (Zeng et al. 2019). Asia, under both current and future climates, harbours large unoccupied areas with high occurrence probabilities for Medfly, whereas Orifly can find large unoccupied suitable areas in South America. Climate change, together with close vicinity of already infested areas (d), will likely drive continued expansions of tephritid species, causing co-invasions of the two species in many areas. The combination of bioclimatic variables, distance to earlier occupied areas and interaction facilitation, could improve the performance of Maxent modelling of invasion dynamics. This modelling protocol, plus incorporating other relevant covariates (e.g. host distributions and dispersal vectors) provide a reliable assessment on the risks and susceptible areas of potential invasion from these fruit fly pests, boosting biosecurity preparedness and preventing future economic losses (Aluja et al. 2008; Suckling et al. 2016; Zhao et al. 2020).

Author contributions

ZZ designed the experiments. ZZ and YZ collected the data and conducted the niche-based model estimation using Maxent. ZZ and CH conducted the statistical analysis and wrote the first draft. ZZ prepared and wrote the original draft manuscript. ZZ, YZ, GA, PH, XP, YQ, ZL, GVPR, MVK and CH reviewed and edited the manuscript. All authors discussed and approved the final version.

Compliance with ethical standards

Funding This study is partially supported by the National Science Foundation of China (No. 31770453).

Conflict of interests The authors declared no competing or financial interests.

Ethical approval This article does not contain any studies with human participants and/or animals (other than insects) performed by any of the authors.

References

Aluja M, Mangan RL (2008) Fruit fly (Diptera: tephritidae) host status determination: Critical conceptual, methodological, and regulatory considerations. Annu. Rev. Entomol 53: 473-502.

Armstrong JW, Tang J, Wang S (2009) Thermal death kinetics of Mediterranean, Malaysian, Melon, and Oriental Fruit Fly (Diptera: Tephritidae) eggs and third instars. J Econ Entomol 102: 522-532.

Bates D, Machler M, Bolker BM, Walker SC (2015) Fitting linear mixed-effects models using lme4. J Stat Softw 67: 1-48.

Beaury EM, Fusco EJ, Jackson MR, Laginhas BB, Morelli TL, Allen JM, Pasquarella VJ, Bradley BA (2020) Incorporating climate change into invasive species management: insights from managers. Biol Invasions 22: 233-252.

Bertelsmeiera C, Ollierb S, Liebholdc AM, Brockerhoffd EG, Warde D, Keller L (2018) Recurrent bridgehead effects accelerate global alien ant spread. PNAS 115: 5486–5491.

Cornelissen B, Neumann P, Schweiger O (2019) Global warming promotes biological invasion of a honey bee pest. Glob Chang Biol 25: 3642-3655.

De Meyer M, Robertson MP, Peterson AT, Mansell MW (2008) Ecological niches and potential geographical distributions of Mediterranean fruit fly (*Ceratitis capitata*) and Natal fruit fly (*Ceratitis rosa*). J Biogeogr 35: 270-281.

De Villiers M, Hattingh V, Kriticos DJ, Brunel S, Vayssieres JF, Sinzogan A, Billah MK, Mohamed SA, Mwatawala M, Abdelgader H, Salah FEE, De Meyer M (2016) The potential distribution of *Bactrocera dorsalis*: considering phenology and irrigation patterns. Bull Entomol Res 106: 19-33.

Dixon P (2003) VEGAN, a package of R functions for community ecology. J Veg Sci 14: 927-930.

Diagne C, Leroy B, Vaissiere AC, Gozlan RE, Roiz D, Jaric I, Salles JM, Bradshaw CJA, Courchamp F (2021) High and rising economic costs of biological invasions worldwide. Nature 592: 571-576.

Elith J, Phillips SJ, Hastie T, Dudik M, Chee YE, Yates CJ (2011) A statistical explanation of MaxEnt for ecologists. Divers Distrib 17: 43-57.

Follett PA, Hennessey MK (2007) Confidence limits and sample size for determining nonhost status of fruits and vegetables to tephritid fruit flies as a quarantine measure. J Econ Entomol 100: 251-257.

Ganie SA, Khan ZH, Ahangar RA, Bhat HA, Hussain B (2013) Population dynamics, distribution, and species diversity of fruit flies on cucurbits in Kashmir Valley, India. J Insect Sci, 13: 65

Godefroid M, Meurisse N, Groenen F, Kerdelhue C, Rossi JP (2020) Current and future distribution of the invasive oak processionary moth. Biol Invasions 22: 523-534.

Hill MP, Bertelsmeier C, Clusella-Trullas S, Garnas J, Robertson MP, Terblanche JS (2016) Predicted decrease in global climate suitability masks regional complexity of invasive fruit fly species response to climate change. Biol Invasions 18: 1105–1119.

Holmes TP, Liebhold AM, Kovacs KF, Von Holle B (2010) A spatial-dynamic value transfer model of economic losses from a biological invasion. Ecol Econ 70: 86-95.

Hui C, Richardson DM (2017) Invasion dynamics. Oxford University Press, Oxford, UK.

Hulme PE (2006) Beyond control: wider implications for the management of biological invasions. J Appl Ecol 43: 835-847.

Hussain MA, Haile A, Ahmad T (2015) Infestation of two tephritid fruit flies, *Bactrocera dorsalis*

(syn. *B. invadens*) and *Ceratitis capitata*, in guava fruits from selected regions of Eritrea. Afr Entomol 23: 510-513.

Kriticos DJ, Kean JM, Phillips CB, Senay SD, Acosta H, Haye T (2017) The potential global distribution of the brown marmorated stink bug, *Halyomorpha halys*, a critical threat to plant biosecurity. J Pest Sci 90: 1033-1043.

Low BW, Zeng YW, Tan HH, Yeo DCJ (2021) Predictor complexity and feature selection affect Maxent model transferability: Evidence from global freshwater invasive species. Divers Distrib 27: 497–511.

Maino JL, Kong JD, Hoffmann AA, Barton MG, Kearney MR (2016) Mechanistic models for predicting insect responses to climate change. Curr Opin Insect Sci 17: 81-86.

Meinshausen M, Smith SJ, Calvin K, Daniel JS, Kainuma MLT, Lamarque JF, Matsumoto K, Montzka SA, Raper SCB, Riahi K, Thomson A, Velders GJM, van Vuuren DPP (2011) The RCP greenhouse gas concentrations and their extensions from 1765 to 2300. Clim Change, 109: 213-241.

Merow C, Smith MJ, Silander JA (2013) A practical guide to MaxEnt for modeling species' distributions: what it does, and why inputs and settings matter. Ecography 36: 1058-1069.

Muscarella R, Galante PJ, Soley-Guardia M, Boria RA, Kass JM, Uriarte M, Anderson RP (2014) ENMeval: An R package for conducting spatially independent evaluations and estimating optimal model complexity for MAXENT ecological niche models. Methods Ecol Evol 5: 1198-1205.

Pearson RG, Raxworthy CJ, Nakamura M, Peterson AT (2007) Predicting species distributions from small numbers of occurrence records: a test case using cryptic geckos in Madagascar. J Biogeog

34: 102-117.

Phillips SJ, Dudik M (2008) Modeling of species distributions with Maxent: new extensions and a comprehensive evaluation. Ecography 31: 161-175.

Pieterse W, Manrakhan A, Terblanche JS, Addison P (2020) Comparative demography of *Bactrocera dorsalis* (Hendel) and *Ceratitis capitata* (Wiedemann) (Diptera: Tephritidae) on deciduous fruit. Bull Entomol Res 110: 185-194.

Pouteau R, Thuiller W, Hobohm C, Brunel C, Conn B, Dawson W, et al (2021) Climate and socio-economic factors explain differences between observed and expected naturalization patterns of European plants around the world. Glob Ecol Biogeogr 30: 1514-1531.

Puchałka R, Dyderski MK, Vitkova M, Sadlo J, Klisz M, Netsvetov M, et al (2021) Black locust (*Robinia pseudoacacia* L.) range contraction and expansion in Europe under changing climate. Glob Chang Biol 27: 1587-1600.

R Core Team (2016) A language and environment for statistical computing. R Foundation for Statistical Computing, Vienna, Austria.

Radosavljevic A, Anderson RP (2014) Making better MAXENT models of species distributions: complexity, overfitting and evaluation. J Biogeogr 41: 629-643.

Rodriguez-Rodriguez SE, Gonzalez-Hernandez H, Rodriguez-Leyva E, Lomeli-Flores JR, Miranda-Salcedo MA (2018) Species diversity and population dynamics of fruit flies (Diptera: Tephritidae) in Guerrero, Mexico. Flo Entomol 101: 113-118.

Seebens H, Briski E, Ghabooli S, Shiganova T, MacIsaac HJ, Blasius B (2019) Non-native species spread in a complex network: the interaction of global transport and local population dynamics determines invasion success. Proc R Soc B-Biol Sci 286: 1901.

Simberloff D, Martin JL, Genovesi P, Maris V, Wardle DA, Aronson J, Courchamp F, Galil B, Garcia-Berthou E, Pascal M, Pysek P, Sousa R, Tabacchi E, Vila M (2013) Impacts of biological invasions: what's what and the way forward. Trends Ecol Evol 28: 58-66.

Stephens AEA, Kriticos DJ, Leriche A (2007) The current and future potential geographical distribution of the oriental fruit fly, *Bactrocera dorsalis* (Diptera : Tephritidae). Bull Entomol Res 97: 369-378

Suckling DM, Kean JM, Stringer LD, Caceres-Barrios C, Hendrichs J, Reyes-Flores J, Dominiak BC (2016) Eradication of tephritid fruit fly pest populations: outcomes and prospects. Pest Manage Sci 72: 456-465.

Szyniszewska AM, Tatem AJ (2014) Global assessment of seasonal potential distribution of Mediterranean fruit fly, *Ceratitis capitata* (Diptera: Tephritidae). PloS one 9: e111582.

Thomas CD (2010) Climate, climate change and range boundaries. Divers Distrib 16: 488–495.

Vera MT, Rodriguez R, Segura DF, Cladera JL, Sutherst RW (2002) Potential geographical distribution of the Mediterranean fruit fly, *Ceratitis capitata* (Diptera: Tephritidae), with emphasis on Argentina and Australia. Environ Entomol 31: 1009-1022.

Warren DL, Seifert SN (2011) Ecological niche modeling in Maxent: the importance of model complexity and the performance of model selection criteria. Ecol Appl 21: 335-342.

Williams JW, Ordonez A, Svenning JC (2021) A unifying framework for studying and managing climate-driven rates of ecological change. Nat Ecol Evol 5: 17–26.

Zeng YY, Reddy GVP, Li ZH, Qin YJ, Wang YN, Pan XB, Jiang F, Gao F, Zhao ZH (2019) Global distribution and invasion pattern of oriental fruit fly, *Bactrocera dorsalis* (Diptera: Tephritidae). J Appl Entomol 143:165-176.

Zhao ZH, Hui C, Plant RE, Su M, Papadopoulos NT, Carpenter TE, Li ZH, Carey JR (2019) The life table invasion models: Spatial progression and species-specific partitioning. Ecology 100: e02682.

Zhao ZH, Reddy GVP, Chen L, Qin YJ, Li ZH (2020) The synergy between climate change and transportation activities drives the propagation of an invasive fruit fly. J Pest Sci 93: 615-625.

437 **Legends**

438 **Figure 1.** Current geographical distributions (up to 2020) of *Bactrocera dorsalis* (Orifly) and
439 *Ceratitis capitata* (Medfly): (a) current occurrence of Orifly; (b) infested countries for Orifly;
440 (c) current occurrence of Medfly, (d) infested countries for Medfly.

441 **Figure 2.** Response curves of bioclimatic variables from the Maxent species distribution models ((a)
442 Temperature Seasonality, (b) Mean Temperature of Warmest Quarter, (c) Mean Temperature of
443 Coldest Quarter, (d) Precipitation of Driest Quarter, (e) Precipitation of Wettest Quarter, and (f)
444 Distance to Infested Area (Invasion Expansion). All probability of presence for both species
445 were indicated with 95% Confidence interval).

446 **Figure 3.** Potential geographical distributions of *Bactrocera dorsalis* (Orifly) and *Ceratitis capitata*
447 (Medfly) under past (1990), present (2020) and future climates (2050 RCP8.5; Earth system
448 model MIROC-ESM-CHEM). (a) Orifly-1990; (b) Orifly-2020; (c) Orifly-2050 RCP8.5; (d)
449 Medfly-1990; (e) Medfly-2020; (f) Medfly-2050 RCP8.5.

450 **Figure 4.** Predicted changes in the potential geographical distributions of (a) *Bactrocera dorsalis*
451 (Orifly) and (b) *Ceratitis capitata* (Medfly) under future climate scenarios (2020-2050 RCP 8.5
452 of MIROC-ESM-CHEM).

453 **Figure 5.** Changes in PGD connectivity (Eqn.6) for *Bactrocera dorsalis* (Orifly) and *Ceratitis*
454 *capitata* (Medfly) in 6 continents by 2050 of RCP 8.5.

455 **Figure 6.** Dominance of *Bactrocera dorsalis* (Orifly) and *Ceratitis capitata* (Medfly) based on
456 occurrence probabilities in the areas where they are predicted to co-occur currently 2020 (a) and
457 in 2050 (b, under RCP8.5 of MIROC-ESM-CHEM).

458

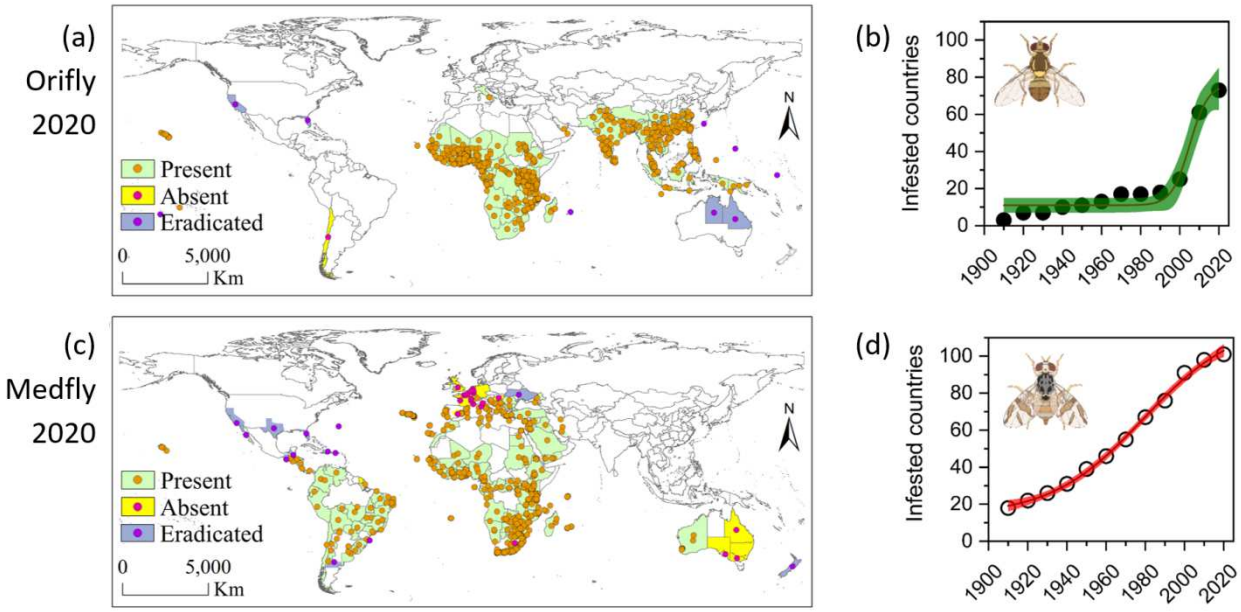
(a)
Orifly
2020
Present
Absent
Eradicated
0
5,000
Km
N
(b)
Infested countries
100
80
60
40
20
0
1900
1920
1940
1960
1980
2000
2020
(c)
Medfly
2020
Present
Absent
Eradicated
0
5,000
Km
N
(d)
Infested countries
100
80
60
40
20
0
1900
1920
1940
1960
1980
2000
2020

Figure 1

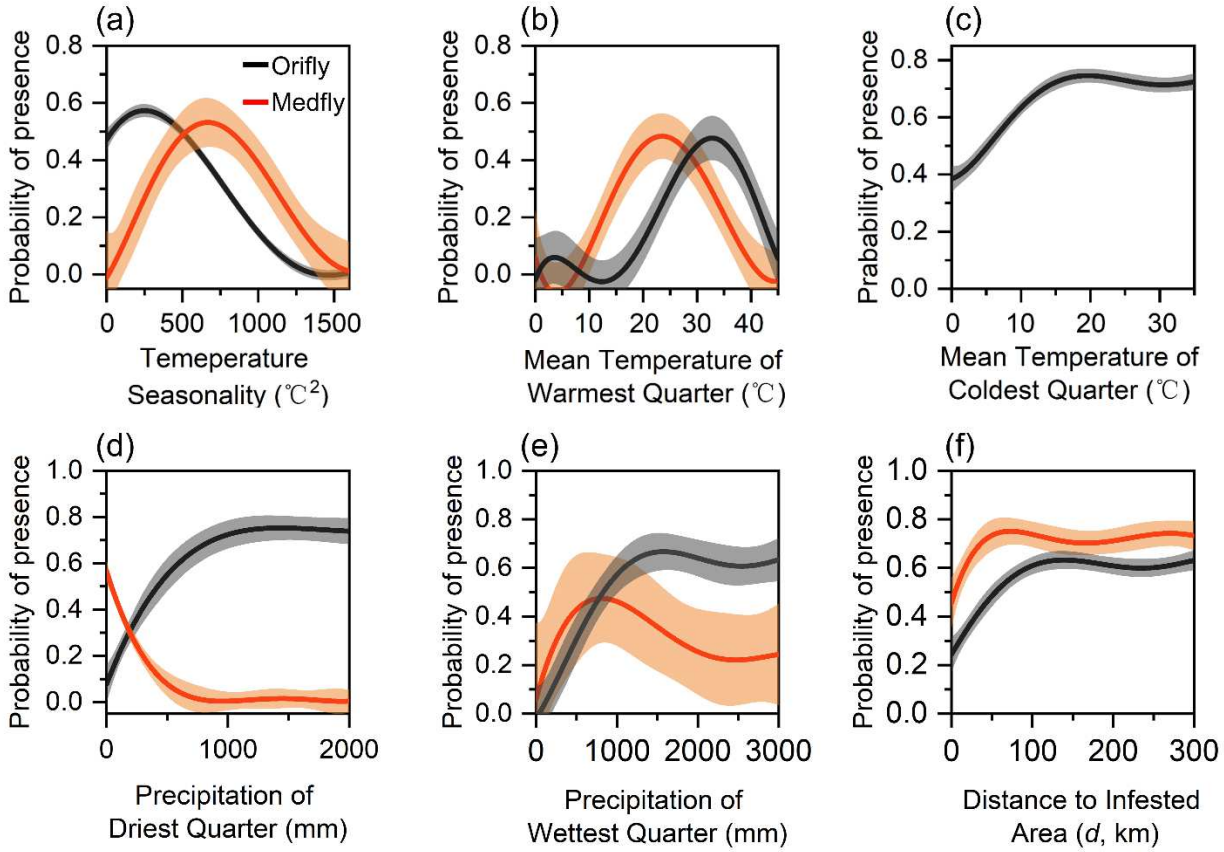
(a)
Orifly
Medfly
Probability of presence
0.0
0.2
0.4
0.6
0.8
0
500
1000
1500
Temeperature
Seasonality (℃^{2})
(b)
Probability of presence
0
10
20
30
40
Mean Temperature of
Warmest Quarter (℃)
(c)
Prabability of presence
Mean Temperature of
Coldest Quarter (℃)
(d)
1.0
2000
Precipitation of
Driest Quarter (mm)
(e)
3000
Precipitation of
Wettest Quarter (mm)
(f)
100
200
300
Distance to Infested
Area (*d*, km)

Figure 2

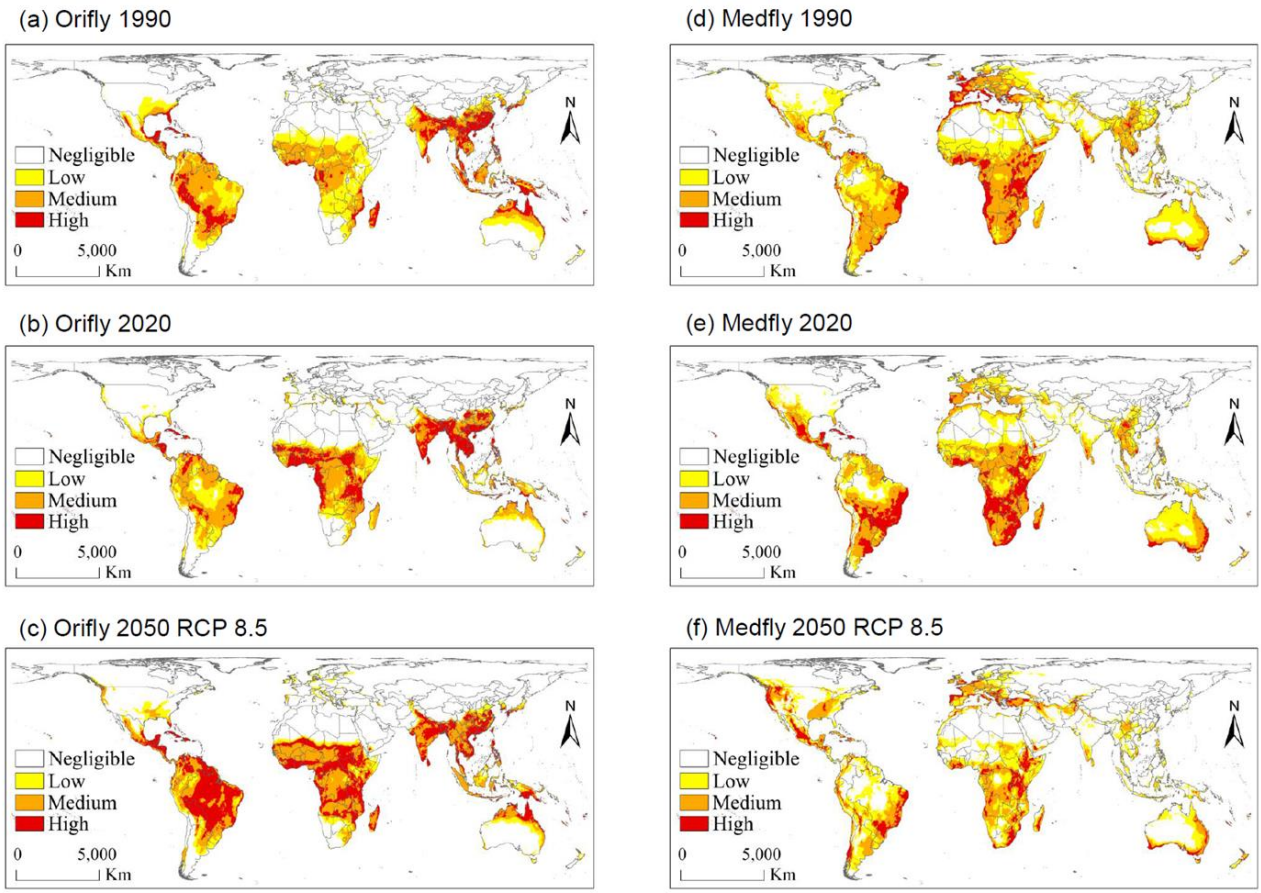
(a) Orifly 1990
(b) Orifly 2020
(c) Orifly 2050 RCP 8.5
(d) Medfly 1990
(e) Medfly 2020
(f) Medfly 2050 RCP 8.5
Negligible
Low
Medium
High
0 5,000
Km
N

Figure 3

(a) Orifly 2020-2050 RCP 8.5

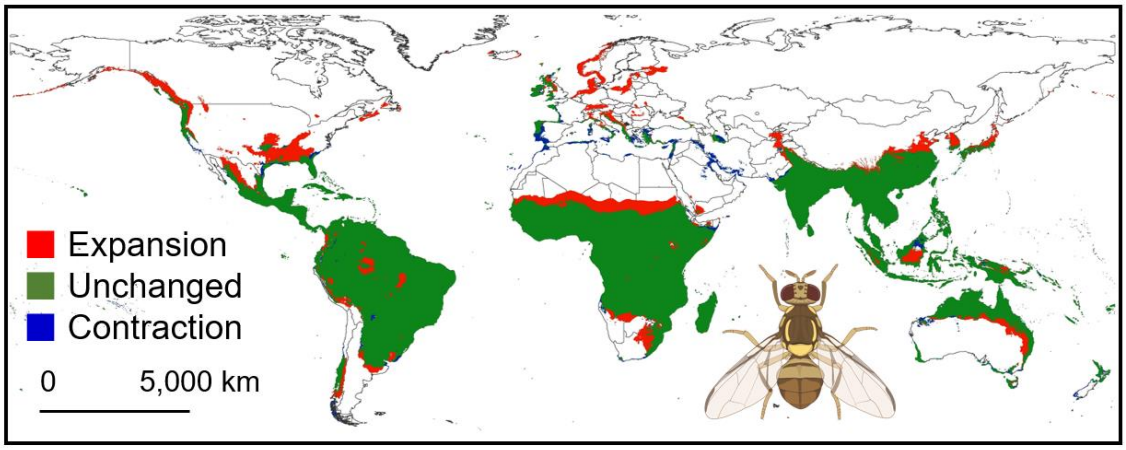

(b) Medfly 2020-2050 RCP 8.5

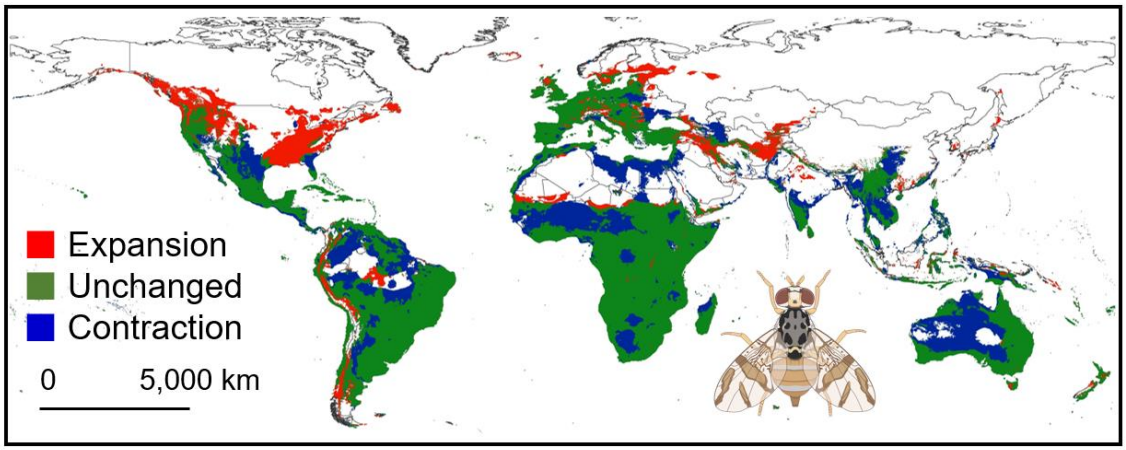

Figure 4

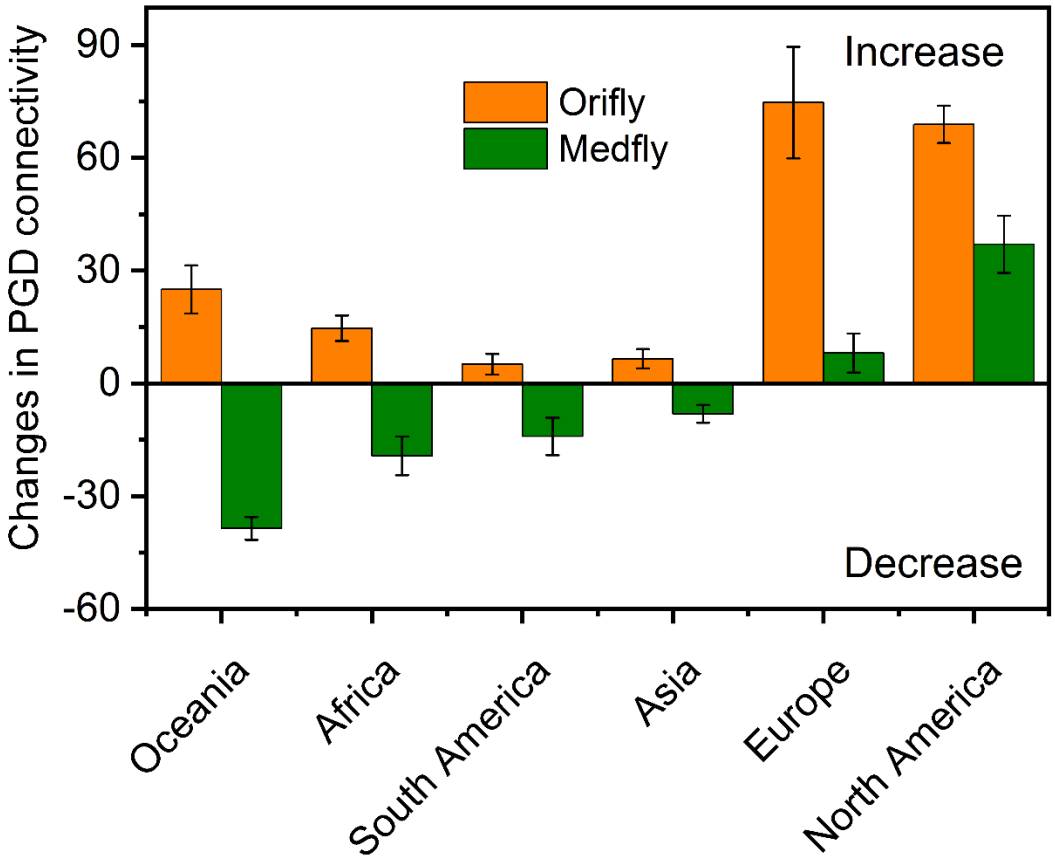
Changes in PGD connectivity
90
60
30
0
-30
-60
Orifly
Medfly
Increase
Decrease
Oceania
Africa
South America
Asia
Europe
North America

Figure 5

(a) Co-occurrence 2020

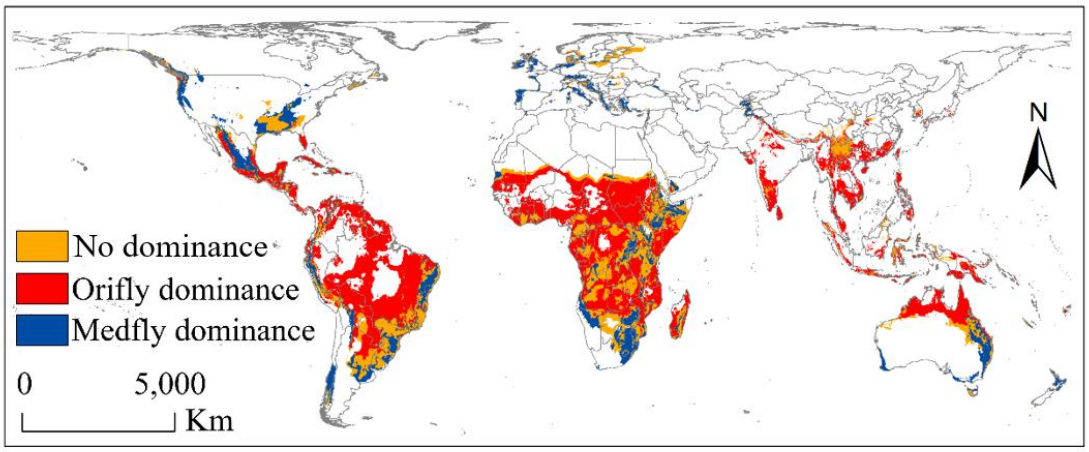

(b) Co-occurrence 2050

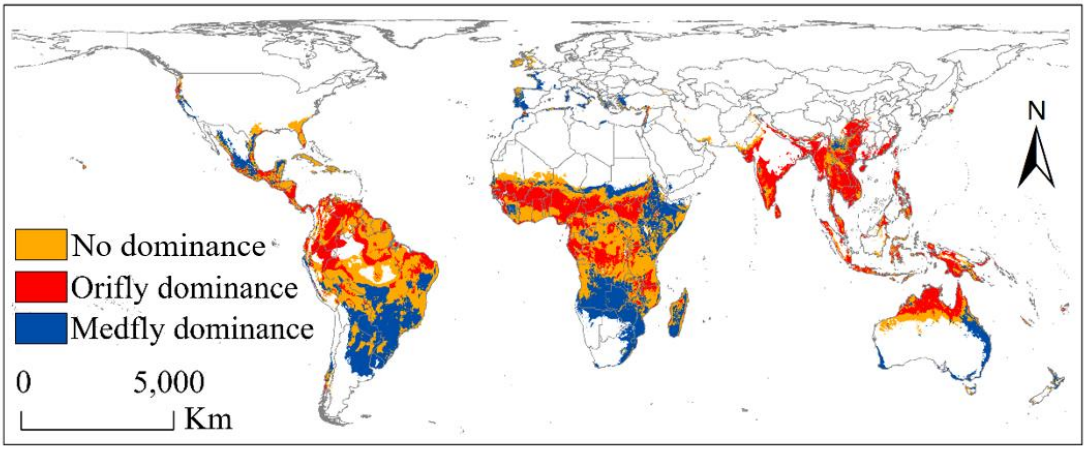

Figure 6

Supplementary Files

This is a list of supplementary files associated with this preprint. Click to download.

- Supplements.docx